

Fluid Mechanics of Microrheology

Todd M. Squires¹ and Thomas G. Mason²

¹Department of Chemical Engineering, University of California, Santa Barbara, California 93106-5080; email: squires@engineering.ucsb.edu

²Department of Chemistry and Biochemistry, Department of Physics and Astronomy, University of California, Los Angeles, California 90095-1569

Annu. Rev. Fluid Mech. 2010. 42:413–38

The *Annual Review of Fluid Mechanics* is online at fluid.annualreviews.org

This article's doi:
10.1146/annurev-fluid-121108-145608

Copyright © 2010 by Annual Reviews.
All rights reserved

0066-4189/10/0115-0413\$20.00

Key Words

rheology, viscoelasticity, Stokes-Einstein relation, mobility, fluctuation dissipation

Abstract

In microrheology, the local and bulk mechanical properties of a complex fluid are extracted from the motion of probe particles embedded within it. In passive microrheology, particles are forced by thermal fluctuations and probe linear viscoelasticity, whereas active microrheology involves forcing probes externally and can be extended out of equilibrium to the nonlinear regime. Here we review the development, present state, and future directions of this field. We organize our review around the generalized Stokes-Einstein relation (GSER), which plays a central role in the interpretation of microrheology. By discussing the Stokes and Einstein components of the GSER individually, we identify the key assumptions that underpin each, and the consequences that occur when they are violated. We conclude with a discussion of two techniques—multiple particle-tracking and nonlinear microrheology—that have arisen to handle systems in which the GSER breaks down.

Complex fluid: a material composed of a liquid base in which supramolecular structures, such as polymers, droplets, or particles, are present

Viscoelasticity: soft materials are neither purely viscous nor purely elastic, and store and dissipate energy in a frequency-dependent way

LVE: linear viscoelastic

Microrheology: study of flow and deformation of very small volumes of materials, typically involving thermal or forced excitations of colloidal probes

Colloidal probe: a structure, such as a particle, droplet, micelle, organelle, or macromolecule, having a size between a nanometer and several micrometers

MSD: mean square displacement

GSER: generalized Stokes-Einstein relation

1. INTRODUCTION

Rheology is the study of how complex materials flow and deform under stress. Complex fluids, such as emulsions, suspensions, polymer, and micellar solutions, play a ubiquitous role in everyday life. They encompass foods, biomaterials, personal care, and industrial products. When such soft materials are strained, their microstructures both store and dissipate the deformation energy in a frequency-dependent manner, reflecting viscoelasticity. The rheological properties of a soft material determine its flow and processing behavior, and provide a window into its microstructural makeup. Traditional rheometers typically measure the frequency-dependent linear viscoelastic (LVE) relationship between strain and stress on milliliter-scale material samples.

Microrheology measures these rheological quantities using colloidal probes directly embedded in a soft material. Rudimentary examples of microrheological measurements date back many decades, when, e.g., Crick & Hughes (1950), Freundlich & Seifriz (1922), and Heilbronn (1922) employed magnetic fields to force iron filings within small biomaterial samples (see Gardel & Weitz 2005 for a review). More recently, well-characterized synthetic magnetic colloids enabled a more quantitative interpretation of the active microrheological experiments of Amblard et al. (1996), Ziemann et al. (1994), and Schmidt et al. (1996) in terms of intrinsic material properties.

A major shift—both in conceptual framework and measurement capabilities—occurred when Mason & Weitz (1995) showed that the equilibrium thermal fluctuations of well-defined colloidal probes were directly related to the local, time-dependent frictional drag or resistance $\zeta(t)$ and thus to the LVE properties of the surrounding soft material. (**Figure 1** depicts a typical experiment.) More specifically, Mason and colleagues (1996, 1997c; Mason & Weitz 1995) used diffusing wave spectroscopy (Weitz & Pine 1993) to measure the mean square displacement (MSD) of fluctuating spherical colloids in concentrated suspensions, spherical colloids in entangled polymer solutions, and droplets in concentrated emulsions. To quantitatively relate the measured MSD of tracer probes to the rheological properties of this broad range of complex fluids, they developed and applied a generalized Stokes-Einstein relation (GSER). In all cases, they found microrheological data to be in excellent agreement with mechanical measurements made via traditional rheometry over a wide frequency range.

In the subsequent decade, a number of innovations expanded the reach and power of microrheological techniques. The light-scattering technique for measuring probe motion used by Mason and colleagues (1996, 1997c; Mason & Weitz 1995) ensemble-averages the statistics of all probes within a measurement volume. Subsequently, Gittes et al. (1997), Mason et al. (1997b), and Schnurr et al. (1997) then used laser microscopy techniques to measure trajectories of individual particles, using the GSER to extract rheological moduli. Kuo & Sheetz (1993) had employed similar techniques to measure the step-wise motion of molecular motors. Although the theoretical approach used by Gittes et al. (1997) and Schnurr et al. (1997) to interpret these measurements seemed distinct from that of Mason and colleagues (1996, 1997c; Mason & Weitz 1995), the two were later reconciled and shown to be equivalent (Mason 2000). Individual probe tracking requires far smaller sample volumes than light scattering (or traditional rheometry) yet yields quantitative data over an extraordinary range of frequencies. Video particle-tracking microscopy, developed largely by Murray & Grier (1996), was then employed for microrheology (Apgar et al. 2000; Crocker et al. 2000; Mason et al. 1997a; Xu et al. 1998a,b). Despite a reduced frequency range, video particle-tracking microrheology techniques grew rapidly, owing to the ready availability of video microscopy capabilities and to the free availability of particle-tracking software due to Crocker, Weeks, and colleagues. Individual particle tracking also enables local material heterogeneity to be probed, giving material information that is completely inaccessible to traditional rheometry. Multiple-particle measurements (Section 5.2) were then introduced (Apgar et al. 2000,

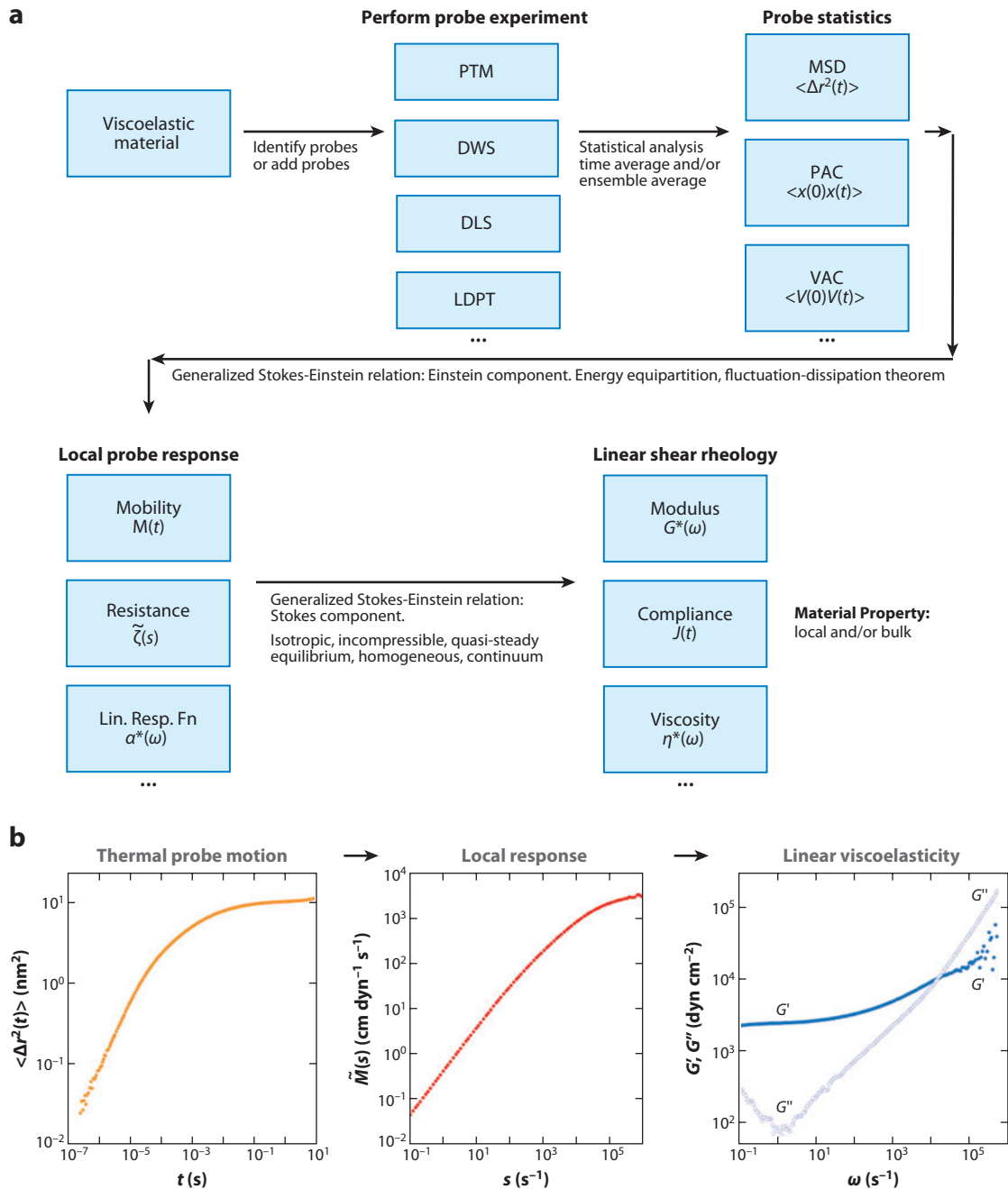


Figure 1

Passive, thermal diffusion microrheology. (a) General scheme for performing and analyzing a passive microrheology experiment, which starts with measured probe trajectories and yields probe mobility and the linear shear viscoelasticity of the complex fluid. (b) Example data and analysis for a concentrated, monodisperse oil-in-water emulsion having average droplet radius 0.52 μm and volume fraction 0.65, as measured using diffusing wave spectroscopy (DWS) (see Mason 2000). DLS, dynamic light scattering; LDPT, laser-deflection particle tracking; MSD, mean square displacement; PAC, positional autocorrelation; PTM, particle-tracking microscopy; VAC, velocity autocorrelation.

Table 1 Experimental methods for measuring probe dynamics

Experimental method	Measured probe dynamics
Scattering methods	
Diffusing wave spectroscopy (DWS)	$\langle \Delta \mathbf{r}^2(t) \rangle, \langle \mathbf{V}(0)\mathbf{V}(t) \rangle$
Dynamic light scattering (DLS)	$\langle \Delta \mathbf{r}^2(t) \rangle, \langle \mathbf{V}(0)\mathbf{V}(t) \rangle$
X-ray photon correlation spectroscopy*	$\langle \Delta \mathbf{r}^2(t) \rangle, \langle \mathbf{V}(0)\mathbf{V}(t) \rangle$
Neutron spin echo*	$\langle \Delta \mathbf{r}^2(t) \rangle, \langle \mathbf{V}(0)\mathbf{V}(t) \rangle$
Fluorescence correlation spectroscopy*	$D(t)$
Real-space methods	
Particle tracking microscopy (PTM)	$x(t), \langle x(0)x(t) \rangle, \langle \Delta x^2(t) \rangle$
Multiparticle tracking microscopy	$x_i(t), \langle x_i(0)x_j(t) \rangle$
Laser-deflection particle tracking	$x(t), \langle x(0)x(t) \rangle$
Particle interferometric tracking (PIT)	$z(t), \langle z(0)z(t) \rangle$
Confocal PTM	$\{x(t), y(t), z(t)\}$
Angular light streak PTM	$\theta(t), \langle \Delta \theta^2(t) \rangle$
Other methods	
Pulsed-field gradient NMR*	$D(t), \langle \Delta r^2(t) \rangle$

*Although these methods have not yet been attempted, they should be useful in microrheology experiments.

Valentine et al. 2001), which enabled heterogeneity mapping, as well as cross-correlated measurements (Crocker et al. 2000) that more effectively recover the macroscopic moduli of heterogeneous materials.

The modern fields of microrheology and microfluidics were not so clearly distinct years ago: Early work on visualizing particle and aggregate flows in microtube microrheology (e.g., Vadas et al. 1973) touched on both fields. Whereas modern microfluidics directs and structures complex fluid flows within submillimeter geometries, modern microrheology is typically concerned with flows around microscale and nanoscale probe particles that are thermally excited or forced using external fields.

The goal of modern microrheology is to extract the rheological properties of a material from the motion of colloidal probes embedded within it. Various realizations of this basic idea have been pursued (**Table 1**). Broad classes include (a) thermal diffusion or passive microrheology, in which the linear-response properties of the material are extracted from the motion of a thermally fluctuating colloidal probe, and (b) active microrheology, in which a probe is actively driven within the material, either in oscillatory or steady motion.

The widespread appeal of microrheology stems from its advantages over traditional rheometry. Particle-tracking microrheology requires very small (e.g., microliter) sample volumes, which enables studies of materials that are either expensive or impossible to acquire in larger quantities, including biomaterials and living cells (see, e.g., reviews by Weihs et al. 2006, Wirtz 2009) and combinatorial studies of material libraries (Breedveld & Pine 2003). Video particle-tracking microrheology requires standard laboratory equipment and can thus be relatively simple experimentally. Laser-based microrheology enables measurements over frequency ranges that far exceed those available to traditional rheometry (Willenbacher & Oelschlaeger 2007). Unlike traditional rheometry, in which each frequency is generally measured separately, passive microrheology employs probe statistics resulting from broadband thermal excitations to effectively measure a wide range of frequencies simultaneously. Passive tracer probes enable measurements to be made with minimal perturbation during the normal processing and evolution of a material or product. Lastly,

Passive

microrheology:

the use of thermal fluctuations of embedded colloidal probes to measure material rheology (also called thermal diffusion microrheology)

Active

microrheology:

the use of externally forced colloidal probes to measure the linear or nonlinear rheological response of a material

local material heterogeneities can be probed directly with colloidal probes, giving information inaccessible to macroscopic rheometry.

Many reviews have detailed the history, practice, and results of microrheology, with expansive reviews given by Waigh (2005), Gardel & Weitz (2005), and Gisler & Weitz (1998). On the theory side, Mason (2000) presents a unified version of what had seemed to be distinct theoretical approaches, and Solomon & Lu (2001) focus on fundamental questions concerning microrheology and its interpretation. Here we examine the development, present state, and future directions of microrheology from its underlying fluid mechanical context. We do so through the lens of the GSER, for which validity is generally assumed, yet not guaranteed. In particular, we review complementary derivations of the GSER, and clearly identify the assumptions that are invoked (Section 2). We then describe the variety of equivalent ways in which the fundamental rheological properties can be encoded—macro, micro, and local probe functions—in Section 3. In Section 4, we discuss situations in which the fundamental assumptions behind the GSER break down, and review the challenges, opportunities, and new techniques that have arisen as a result. Finally, we give a detailed discussion in Section 5 of two new techniques—multiparticle and nonlinear microrheology—that have been developed in response to a breakdown of the GSER.

2. THE GENERALIZED STOKES-EINSTEIN RELATION

Traditional (macroscopic) rheometers enable direct mechanical measurements of the frequency-dependent complex shear modulus $G^*(\omega)$, defined by the linear relationship

$$\tau_0 e^{i\omega t} = G^*(\omega) \gamma_0 e^{i\omega t}, \quad (1)$$

between a weak oscillatory shear stress having magnitude τ_0 and a small oscillatory shear strain having magnitude γ_0 . Mason & Weitz (1995) extracted these same rheological properties from the thermal motion of colloidal probes embedded within the material, giving the first demonstration of thermal diffusion microrheology. Several generalizing assumptions, encapsulated in the GSER, enable the quantitative interpretation of such measurements.

In what follows, we present the original derivation of this fundamentally important relation, due to Mason & Weitz (1995), as well as an alternate but equivalent approach for the Einstein component due to Gittes et al. (1997). We clearly delineate the assumptions that underpin the Einstein and Stokes components, and the rather general conditions under which they can be expected to hold.

For intuition's sake, we begin by discussing the simplest possible experiment in microrheology: diffusion of a spherical colloid of radius a in a Newtonian fluid. The colloid's diffusivity D can be obtained from the MSD ($\langle \Delta x^2(t) \rangle = 2Dt = 2D\tau$), which can be measured by various means (Table 1). The desired rheological property is the viscosity η , which can be extracted from D using two key ideas. First, Einstein (1905) and Sutherland (1905) showed that the diffusivity D of a particle can be related to its hydrodynamic mobility M , defined by $\mathbf{U} = M\mathbf{F}$. Namely, detailed balance requires the net probability flux \mathbf{j} to vanish in equilibrium, so that a particle in a potential field Φ obeys

$$\mathbf{j} = -D\nabla P - (M\nabla\Phi)P = 0, \quad (2)$$

where P is the probability density function for the particle. In equilibrium, Equation 2 is solved quite generally by the Boltzmann distribution $P = P_0 \exp(-\Phi/k_B T)$, so long as

$$D = k_B T M. \quad (3)$$

This is the simplest version of the Einstein component of the GSER, which relates a thermal, stochastic property (diffusivity) to a deterministic, mechanical property (mobility). Equation 3 is

Complex shear modulus: frequency-dependent ratio between oscillatory stress and strain, composed of in-phase, real, storage component G' and out-of-phase, imaginary, loss component G''

Hydrodynamic mobility: frequency-dependent ratio of velocity to force of a probe excited in a soft material: $M^*(\omega) = M'(\omega) + iM''(\omega)$

Einstein component: an assumed relation between thermal fluctuations and deterministic probe mobility, which underpins the GSER and is valid for equilibrium systems

Stokes component: an assumed relation that underpins the GSER and relates probe mobility to complex shear modulus

FDT: fluctuation-dissipation theorem

GSM: generalized Stokes mobility

not limited to individual spherical colloids, but holds for probes of arbitrary shape and complexity, albeit with tensorial $\vec{\vec{D}}$ and $\vec{\vec{M}}$. Additionally, Batchelor (1976) generalized Equation 3 to account for multiparticle systems with hydrodynamic interactions.

The Stokes component of the GSER then relates the deterministic probe response (mobility) to the rheological properties of the material. To do so, the Stokes equations for Newtonian fluids are solved around a spherical probe to yield the Stokes mobility $M_S = (6\pi\eta a)^{-1}$. The resulting Stokes-Einstein relation,

$$D = \frac{k_B T}{6\pi\eta a}, \quad (4)$$

thus connects the measured MSD to the material's viscosity η .

The key insight that launched modern microrheology occurred when Mason & Weitz (1995) showed, theoretically and experimentally, that this strategy could be generalized to treat non-Newtonian materials. In doing so, two significant complications arise. First, the simple detailed balance argument Einstein used for viscous fluids is not obviously applicable for complex fluids with frequency-dependent response properties. The Einstein component, however, can be generalized using the fluctuation-dissipation theorem (FDT) (see Reif 1965 or Landau & Lifshitz 2000) to relate the thermal fluctuations of the probe directly to the frequency-dependent complex mobility $M^*(\omega)$. Second, relating a probe's mobility $M^*(\omega)$ to the complex viscosity $\eta^*(\omega)$, or the complex shear modulus $G^*(\omega) = i\omega\eta^*(\omega) = G'(\omega) + iG''(\omega)$, is not necessarily straightforward, because the (unknown) rheological properties of the material are required even to pose the fluid mechanical problem to be solved. Instead, a crucial assumption is made to generalize the Stokes component of the GSER: namely, that the generalized Stokes mobility (GSM) $M^*(\omega)$ and resistance $\zeta^*(\omega)$ are given precisely by their Newtonian analogs, but with the Newtonian viscosity η replaced by the material's frequency-dependent complex viscosity $\eta^*(\omega)$:

$$M^*(\omega) = \frac{\eta_0}{\eta^*(\omega)} M_S, \quad \text{or} \quad \zeta^*(\omega) = \frac{\eta^*(\omega)}{\eta_0} \zeta_S. \quad (5)$$

2.1. The Hydrodynamic Mobility

The fundamental quantity measured in probe-based microrheology is the mobility M of a probe in a given material, whether in response to an externally applied force (active microrheology) or to stochastic thermal forces (passive microrheology). Following Zwanzig & Bixon (1970), the hydrodynamic mobility M and resistance ζ are generalized for LVE materials according to

$$V(t) = \int_{-\infty}^t M(t-t') F_H(t') dt' \quad \text{and} \quad F_H(t) = \int_{-\infty}^t \zeta(t-t') V(t') dt', \quad (6)$$

where F_H is the hydrodynamic force on the particle. The Laplace transform (denoted with tildes) of Equation 6 reveals the transform of each to be the inverse of the other,

$$\tilde{V}(s) = \tilde{\zeta}^{-1}(s) \tilde{F}(s) \equiv \tilde{M}(s) \tilde{F}(s), \quad \text{so} \quad \tilde{M}(s) = \tilde{\zeta}^{-1}(s), \quad (7)$$

where s is the Laplace frequency.

2.2. The Einstein Component

The Einstein component of the GSER relates the thermal fluctuations of a probe to its mechanical response [mobility $M^*(\omega)$ in the material] and is typically derived via two equivalent routes.

Mason & Weitz (1995) employed the generalized Langevin equation,

$$m\dot{V}(t) = f_R(t) - \int_0^t \zeta(t-t')V(t')dt', \quad (8)$$

for a spherical probe subject to a weak stochastic force $f_R(t)$ in an isotropic LVE material. Here m and V are the mass and velocity of the probe, respectively. The Laplace transform of Equation 8 can be solved for $\tilde{V}(s)$ to obtain

$$\tilde{V}(s) = \frac{mV(0) + \tilde{f}_R(s)}{ms + \tilde{\zeta}(s)}. \quad (9)$$

Because f_R is stochastic, $V(t)$ must be treated statistically. Multiplying Equation 9 by $V(0)$ and computing the ensemble average of both sides, denoted $\langle \cdot \rangle$, give a velocity autocorrelation function (VAC):

$$\langle V(0)\tilde{V}(s) \rangle = \frac{\langle V(0)\tilde{f}_R(s) \rangle + m\langle V(0)^2 \rangle}{ms + \tilde{\zeta}(s)}. \quad (10)$$

Mason & Weitz (1995) then employed two key facts from equilibrium statistical mechanics (see, e.g., Landau & Lifshitz 2000, Reif 1965). First, the stochastic thermal force f_R is uncorrelated with the velocity of the probe: $\langle f_R V \rangle = 0$, where angular brackets denote ensemble averages. Second, the equipartition theorem states that each quadratic degree of freedom has an average of $\frac{1}{2}k_B T$ of energy, so that the kinetic energy $\frac{1}{2}m\langle V(0)^2 \rangle = \frac{1}{2}k_B T$ for unidirectional motion. The VAC for N -dimensional probe translation is thus

$$\langle V(0)\tilde{V}(s) \rangle = \frac{Nk_B T}{ms + \tilde{\zeta}(s)}. \quad (11)$$

Typical microrheology experiments are performed at low enough frequencies that the resistance $\tilde{\zeta}(s)$ dominates over probe inertia ms , so that

$$\langle V(0)\tilde{V}(s) \rangle \approx Nk_B T\tilde{\zeta}^{-1}(s) = Nk_B T\tilde{M}(s). \quad (12)$$

Finally, the VAC can be related to the MSD via the identity

$$\langle V(0)\tilde{V}(s) \rangle = \frac{s^2}{2}\mathcal{L}\langle \Delta \mathbf{r}^2(t) \rangle \equiv \frac{s^2}{2}\langle \Delta \tilde{\mathbf{r}}^2(s) \rangle, \quad (13)$$

where \mathcal{L} denotes the Laplace transform operator, to give

$$\langle \Delta \tilde{\mathbf{r}}^2(s) \rangle \approx \frac{2Nk_B T}{s^2\tilde{\zeta}(s)} \equiv \frac{2Nk_B T}{s^2}\tilde{M}(s), \quad (14)$$

or

$$\tilde{M}(s) \approx \frac{s^2\langle \Delta \tilde{\mathbf{r}}^2(s) \rangle}{2Nk_B T}. \quad (15)$$

The (measurable) MSD is thus directly related to the mobility of the probe in the material of interest.

An alternate, but equivalent, approach was pursued by Gittes et al. (1997), Schnurr et al. (1997), and MacKintosh & Schmidt (1999), who worked with a linear-response function $\alpha(t)$ that relates probe displacement to a weak applied force $F(t)$,

$$r(t) - r(0) = \int_0^t \alpha(t-\tau)F(\tau)d\tau, \quad (16)$$

neglecting probe inertia. The bilateral Fourier transform (with operator denoted \mathcal{F}^b and transformed functions by *b) of $\alpha(t)$ is related to the mobility via $\alpha^{*b}(\omega) = M^{*b}(\omega)/(i\omega)$. The FDT

VAC: velocity autocorrelation function

PSD: power spectral density

relates the power spectral density (PSD) $S^r(\omega)$ to the imaginary part of $\alpha^{*b}(\omega)$ [i.e., the viscous (dissipative) component $M(\omega)$ of the mobility] via

$$S^r(\omega) \equiv \mathcal{F}^b \langle r(0)r(\tau) \rangle = \frac{2k_B T}{\omega} \Im(\alpha^{*b}(\omega)) \equiv -\frac{2k_B T}{\omega^2} \Re(M^{*b}(\omega)). \quad (17)$$

Here \Im and \Re denote the imaginary and real parts. The elastic component, $M'(\omega)$, can be obtained directly from $M(\omega)$ using the Kramers-Kronig relations (see, e.g., Landau & Lifshitz 2000a, Reif 1965).

Although these two routes to (and representations of) the GSER may appear different, the information they contain is identical. Mason (2000) emphasized this point by deriving a variety of analogous, and equivalent, representations of the essential concept captured by the GSER. For example, unilateral Fourier transforms can be used in place of Laplace transforms in Equations 8–15 to yield

$$\mathcal{F}^u \langle \Delta r(0)\Delta r(t) \rangle = \int_0^\infty \langle \Delta r(0)\Delta r(t) \rangle e^{-i\omega t} dt = -\frac{2k_B T}{\omega^2} M^{*u}(\omega), \quad (18)$$

whereas bilateral Fourier transforms recover Equation 17 exactly.

The Einstein part of the GSER thus relates a stochastic quantity (thermal fluctuations) to a deterministic one (the linear response of a probe under weak oscillatory forcing). Experimentally, then, the Einstein part allows the (transformed) mobility $\tilde{M}(s)$ to be extracted from the (transformed) MSD or the PSD, which can be measured using dynamic light scattering (e.g., Berne & Pecora 2000), particle tracking, and other techniques (**Table 1**).

2.3. The Stokes Component

The Stokes component of the GSER relates the complex mobility $M^*(\omega)$ of a probe to the rheological properties of the material in which it resides. To properly do so, the hydrodynamic equations appropriate for the material must be solved around an oscillatory probe. However, because the constitutive equations for the material represent the unknown (and desired) quantity, the Stokes component would generally require the inverse problem to be solved. Instead, the GSM form (Equation 5) has been historically assumed for $M^*(\omega)$. With this assumption, this Stokes and Einstein components (Equation 14) combine to give the GSER.

The most commonly measured quantity in microrheology is the translational diffusion of spherical colloids, whose mobility is assumed to generalize via $M^*(\omega) = (6\pi\eta^*(\omega)a)^{-1}$, giving a GSER

$$\langle \Delta \tilde{r}^2(s) \rangle = \frac{Nk_B T}{3\pi a s^2 \tilde{\eta}(s)} = \frac{Nk_B T}{3\pi a s \tilde{G}(s)}, \quad (19)$$

where N is the number of dimensions tracked in the MSD and $\tilde{G}(s)$ is the Laplace-transformed complex shear modulus. Analogous versions of the GSER for other probe shapes and motions require the relevant Stokes mobility problem to be solved. For example, Bishop et al. (2004) tracked the rotation of spherical colloids,

$$\langle \Delta \tilde{\theta}^2(s) \rangle = \frac{k_B T}{4\pi a^3 s^2 \tilde{\eta}(s)} = \frac{k_B T}{4\pi a^3 s \tilde{G}(s)}, \quad (20)$$

where $\langle \Delta \tilde{\theta}^2(s) \rangle$ is the Laplace-transformed mean-squared angular displacement. Cheng & Mason (2003) tracked the rotation of an obliquely rotating disk, for which the drag calculation of Zhang & Stone (1998) gives the GSER to be

$$\langle \Delta \tilde{\theta}^2(s) \rangle = \frac{3k_B T}{16\pi a^3 s^2 \tilde{\eta}(s)} = \frac{3k_B T}{16\pi a^3 s \tilde{G}(s)}. \quad (21)$$

INTERFACIAL MICRORHEOLOGY

Just as complex microstructures impart interesting rheological properties to bulk materials, surface-active species (surfactants) can confer nontrivial dynamical properties to fluid-fluid interfaces. The rheology of such interfaces can play an important role in interfacial dynamics, including the drainage of foams, coarsening of emulsions, and diffusion of membrane proteins on cell membranes (e.g., Edwards et al. 1991). However, measurements of the complex interfacial viscosity η_s^* can be particularly challenging due to the (often) molecularly thin nature of the interface, as interfacial effects can be overwhelmed by the bulk fluid(s) on either side. The interfacial contribution to the drag on a probe is exerted along the contact perimeter P_c , whereas the bulk contribution is exerted over the contact area A_c . The dimensionless Boussinesq number,

$$Bo = \frac{\eta_s^* P_c}{\eta^* A_c},$$

which expresses their relative importance, must be large to accurately measure interfacial rheology, such that the high P_c/A_c ratio of colloidal probes makes interfacial microrheology a particularly sensitive technique. Interesting hydrodynamic challenges arise in interfacial microrheology, including multiple length scales (e.g., Henle et al. 2008, Saffman & Delbruck 1975, Stone & Ajdari 1998), interfacial compressibility (Fischer 2004, Sickert et al. 2007), and the transition between two-dimensional (singular) Stokes flows and well-behaved three-dimensional flows (Prasad & Weeks 2009).

Given the sensitive dependence of the rotational GSER on particle size and shape, these quantities must be measured accurately to extract $\tilde{G}(s)$ from rotational fluctuations.

In the development of microrheology, however, the GSM has remained effectively an assumption. Its success is amply evident in many cases, yet it does not hold universally. Xu et al. (2007) and Schnurr et al. (1997) attribute its frequent success to the fact that the Fourier-transformed equations of motion for incompressible LVE materials are identical to Stokes equations (i.e., the classic viscous-viscoelastic analogy). Indeed, it can be shown explicitly and quantitatively that the GSM (Equation 5) holds for any probe motion in a simple LVE material under conditions of quasi-steady deformations, material continuum, homogeneity, isotropy, and incompressibility (T.M. Squires & T.G. Mason, manuscript in preparation).

To confidently use the GSER to extract the LVE properties of soft materials, one must ensure that both the Stokes and Einstein components hold for the particular soft material and probe. Comparisons with macroscopic rheometry have shown the straightforward application of the GSER to be quite reliable for microscale probes in isotropic, homogeneous soft materials wherein nanoscale structures provide an elastic response. Examples include entangled polymer solutions, such as aqueous poly(ethylene oxide) (Dasgupta et al. 2002, Mason & Weitz 1995, van Zanten et al. 2004) and concentrated solutions of semiflexible biopolymers such as DNA whose persistence lengths are short compared to the probe size (Mason et al. 1997b). Likewise, excellent agreement has been shown over a wide frequency range for homogeneous micellar solutions (Atakhorrami & Schmidt 2006, Cardinaux et al. 2002, Willenbacher et al. 2007). The GSER has been applied to dense colloidal dispersions that form isotropic disordered glasses, such as repulsive hard sphere and droplet suspensions (Mason & Weitz 1995), as well as nanoscale particulate clays, such as laponite (Bellour et al. 2003, Harden & Viasnoff 2001, Jabbari-Farouji et al. 2007). Many other materials and applications have been demonstrated.

Although the simple application of the GSER has been shown to be valid for many kinds of soft materials, there are some materials for which naively applying the GSER could lead to inaccurate

Creep compliance: viscoelastic response of a material to a step change in stress, given by the strain evolution divided by the stress magnitude

results. If glasses exhibit significant dynamical heterogeneity or are formed through attractive jamming, the naive application of the GSER may yield only approximate results, and multiparticle visualization and cross-correlation techniques may be necessary to extract a meaningful viscoelastic response. Solutions of semiflexible biopolymers that have persistence lengths comparable to or larger than the probe size, such as F-actin (Gardel et al. 2003, Gisler & Weitz 1999, Gittes et al. 1997, Schmidt et al. 2000), can violate the assumptions of the simple GSER because the probe alters the local structure of the polymer near itself. Obviously, active and living materials, which have nonthermal driving forces and intermittent dynamics, lie beyond the scope of the simple GSER, and the interpretation of these more complex dynamics, for which thermal driving plays only a partial role, is the main subject of the frontier of biomicro-rheology (Weihs et al. 2006).

3. EQUIVALENT REPRESENTATIONS OF THE GENERALIZED STOKES-EINSTEIN RELATION

Above we discuss the GSER in terms of the complex, frequency-dependent viscosity $\eta^*(\omega)$, which contains both the elastic and viscous response. The complex viscosity is but one of a number of entirely equivalent ways of representing the LVE behavior, as described by Bird et al. (1987), Larson (1999), and Macosko (1994). One can equally well cite the complex shear modulus $G^*(\omega) = i\omega\eta^*(\omega) = G'(\omega) + iG''(\omega)$, where $G'(\omega)$ and $G''(\omega)$ are the storage and loss moduli, respectively. The complex viscosity $\eta^*(\omega)$ and the complex shear modulus $G^*(\omega)$ are the Fourier transforms of the stress relaxation modulus $G_r(t)$ and memory function $M_r(t-t') = \partial G_r(t-t')/\partial t'$, respectively, which relate stress to strain-rate history or strain history via

$$\tau(t) = - \int_{-\infty}^t G_r(t-t')\dot{\gamma}(t')dt', \quad (22)$$

$$\tau(t) = \int_{-\infty}^t M_r(t-t')\gamma(t')dt', \quad (23)$$

where the response of real materials is causal [i.e., $G_r(t < 0) = M_r(t < 0) = 0$]. All are entirely equivalent ways of representing the same information; thus, the GSER can be expressed in a variety of equivalent forms, summarized in **Table 2**.

A convenient representation of the GSER involves the creep compliance $J(t)$, which is the time-dependent strain following a suddenly applied weak shear stress,

$$\Theta(t) = \int_{-\infty}^t M_r(t-t')J(t')dt', \quad (24)$$

where $\Theta(t)$ is the Heaviside step function. Using the Laplace transform of Equation 24, $s^{-1} = \tilde{G}(s)\tilde{J}(s)$, the GSER (e.g., Equation 19) can be re-expressed in the time domain as

$$\langle \Delta \mathbf{r}^2(s) \rangle = \frac{Nk_B T}{3\pi a} \tilde{J}(s), \quad \text{or} \quad \langle \Delta \mathbf{r}^2(t) \rangle = \frac{Nk_B T}{3\pi a} J(t). \quad (25)$$

That is, the MSD of a spherical probe is directly proportional to the macroscopic creep compliance of the material (Xu et al. 1998a).

Although the information contained in these representations may be identical, each has advantages and disadvantages when dealing with actual data. For example, noisy or incomplete data complicate the numerical inversion of the Laplace transform in Equation 19, particularly at the frequency extremes of a limited data set (e.g., Savin & Doyle 2005). Instead, Mason & Weitz (1995) fitted the measured $\tilde{G}(s)$ to a functional form, and then used analytic continuation (swapping Laplace for Fourier frequency, $s \rightarrow i\omega$) to recover $G'(\omega)$ and $G''(\omega)$. Mason (2000) derived an approximate method to recover $G'(\omega)$ and $G''(\omega)$ from the log slope of the MSD, without numerical

Table 2 Connecting macroscopic linear rheology and probe dynamics with thermal diffusion (passive) microrheology

Property	Symbol	Relation
Linear shear rheology		
Complex shear modulus	$G^*(\omega)$	$\tau(\omega) = G^*(\omega)\gamma(\omega)$
Complex viscosity	$\eta^*(\omega)$	$G^*(\omega) = i\omega\eta^*(\omega)$
Stress relaxation modulus	$G_r(t)$	$\tau(t) = -\int_{-\infty}^t G_r(t-t')\dot{\gamma}(t')dt'$
Creep compliance	$J(t)$	$\Theta(t) = \int_{-\infty}^t M_r(t-t')J(t')dt'$
Local probe response		
Probe mobility	$M(t)$	$V(t) = \int_0^t M(t-t')F(t')dt'$
Probe resistance	$\zeta(t)$	$F(t) = \int_0^t \zeta(t-t')V(t')dt'$
	$\tilde{\zeta}(s) = \tilde{M}^{-1}(s)$	
Linear-response function	$\alpha^*(\omega)$	$M^*(\omega) = i\omega\alpha^*(\omega)$
Local transfer function	$\tilde{\alpha}(s)$	$\tilde{M}(s) = s\tilde{\alpha}(s)$
Probe statistics		
Mean square displacement (MSD)	$\langle \Delta \mathbf{r}^2(t) \rangle$	$\mathcal{L}\langle \Delta \mathbf{r}^2 \rangle = \frac{2Nk_B T}{s^2} \tilde{M}(s)$
Positional autocorrelation (PAC)	$\langle x(0)x(t) \rangle$	$\mathcal{L}\langle x(0)x(t) \rangle = \frac{2k_B T}{s^2} \tilde{M}(s)$
Power spectral density (PSD)	$S^x(\omega) = \mathcal{F}\langle x(0)x(t) \rangle$	$S^x(\omega) = \frac{2k_B T\alpha''(\omega)}{\omega}$
Velocity autocorrelation (VAC)	$\langle V(0)V(t) \rangle$	$\langle V(0)\tilde{V}(s) \rangle = \frac{s^2 \langle \Delta \mathbf{r}^2(s) \rangle}{2}$
Time-dependent diffusivity	$D(t)$	$\frac{d\langle \Delta \mathbf{r}^2(t) \rangle}{dt} = 2ND(t)$
Two-point (coupling) MSD	$\langle \Delta x_1(0)\Delta x_2(t) \rangle$	$\mathcal{L}\langle \Delta x_1(0)\Delta x_2(t) \rangle = \frac{2k_B T}{s^2} \tilde{M}_{12}(s)$

Macroscopic shear rheology \longleftrightarrow flow field \longleftrightarrow local probe response \longleftrightarrow fluctuation-dissipation theorem \longleftrightarrow probe statistics.

inversions, which Dasgupta and colleagues (2002) improved by accounting for curvature. By contrast, PSD measurements are naturally performed in Fourier space, which in principle obviates the need to transform the data. However, the PSD only measures the imaginary (lossy) part of $\alpha^{*b}(\omega)$ directly, so that Kramers-Kronig integrals must be evaluated with noisy and finite data sets to recover the real part. Evans et al. (2009) have presented a method for converting creep compliance $J(t)$ (and therefore MSD, via Equation 25) into $G'(\omega)$ and $G''(\omega)$ directly, without transforms.

4. WHEN THE GENERALIZED STOKES-EINSTEIN RELATION BREAKS DOWN

Above we discuss the GSER—the central idea of modern microrheology. The generality with which it holds has enabled quantitative microrheological measurements of an incredibly wide range of materials, over a wide range of frequencies, and in a wide range of conditions.

There are cases, however, in which at least one of the key assumptions—involving either the Stokes or Einstein component—fails. In such cases, one can not generally expect agreement between microscopic and macroscopic measurements. In some cases, however, such failures encode new rheological information that is inaccessible to macroscopic rheometry. In other cases, failures have motivated the development of new techniques. It is thus important to understand which assumptions are violated and what can be learned when they are.

4.1. How the Einstein Component Can Break Down

The Einstein component of the GSER follows directly from equilibrium statistical mechanics and is thus valid quite generally so long as the system is in equilibrium. Therefore, the only instances

in which the Einstein part breaks down involve systems that are forced out of equilibrium in some way. Three notable cases stand out: (a) probes that are actively forced through the material strongly enough to drive the material out of equilibrium; (b) materials that are themselves active, i.e., consume chemical energy to produce mechanical stresses; and (c) nonequilibrium materials that are evolving.

4.1.1. Forced probes: active microrheology. In active microrheological experiments, an external force is used to drive a probe through a material. Under conditions of sufficiently gently forcing, both the Stokes and Einstein components remain valid, although the linear response $M^*(\omega)$ is measured directly without recourse to the FDT. This is valuable for stiffer materials, as probes may be actively driven strongly enough to elicit a measurable response (Gardel & Weitz 2005, Waigh 2005) and enable lock-in detection (Valentine et al. 1996). Furthermore, active techniques complement passive ones to enable direct tests of the FDT in nonequilibrium materials (e.g., Harden & Viasnoff 2001, Hoffman et al. 2006, Jabbari-Farouji et al. 2007, Mizuno et al. 2007). Conversely, active forcing may inadvertently drive a nonlinear probe response, as can be checked with a force sweep. Furthermore, mobilities must be measured one frequency at a time, as opposed to thermal fluctuations, which excite all frequencies simultaneously.

Actively-forced probes date back nearly a century (reviewed, e.g., in Waigh 2005 and Gardel & Weitz 2005), and modern variants enable precise quantitative measurements (e.g., Bausch et al. 1998; Schmidt et al. 1996, 2000; Valberg & Albertini 1985; Ziemann et al. 1994). Laser tweezers can exert optical forces on colloidal probes with higher spatial addressability, but weaker magnitude, than magnetic forces (Furst 2005). Probe mobilities have been measured in response to an applied force (Sriram et al. 2009, Valentine et al. 1996, Velegol & Lanni 2001), to an oscillatory force on an adjacent probe (e.g., Atakhorrami et al. 2008b, Hough & Ou-Yang 2002), and to a steady force (Lugowski et al. 2002, Meyer et al. 2006). The oscillatory measurements of Sriram et al. (2009) in colloidal suspensions, for example, showed excellent agreement with both mechanical rheometry and explicit linear-response calculations of the colloidal response.

A sufficiently strong force, conversely, can drive the material out of equilibrium and probe its nonlinear response. A challenge for the theory and interpretation of nonlinear microrheology is the inherently nonequilibrium state of the microstructure, which must be determined to relate the mobility to the underlying rheology. This stands in direct contrast to passive, linear-response systems, in which the Stokes component can be shown to hold under rather general conditions, without explicit calculations. We discuss active nonlinear microrheology in detail in Section 5.2.

4.1.2. Active materials. The Einstein component can also fail with materials that are themselves active, as occurs in biopolymer networks driven by motor proteins (Fletcher & Geissler 2009, Liverpool et al. 2001, MacKintosh & Levine 2008, Nedelec et al. 1997). For example, Mizuno et al. (2007, 2008) measured probe mobility $M^*(\omega)$ in a cross-linked actin network in the presence of the molecular motor myosin, which generates a relative sliding between filaments in the presence of the chemical fuel adenosine triphosphate (ATP). They did so in two ways: actively, with a weak oscillatory applied force, and passively, by measuring the fluctuating trajectory of the probe. If the material were in equilibrium, the FDT would unequivocally relate the two via Equation 17, which did indeed occur in the absence of ATP. When ATP was added, however, Equation 17 was violated at low frequencies (<10 Hz), with extra power in the low-frequency fluctuations provided by the motor activity. Comparisons of the active and passive probe response, for example, reveal much about the mechanical behavior of living cells (Brunner et al. 2009, Gallet et al. 2009, Hoffman et al. 2006, Martin et al. 2001, Weihs et al. 2006, Wilhelm 2008, Wirtz 2009).

4.1.3. Evolving and aging materials. In principle, a material that is evolving toward equilibrium renders the FDT inapplicable. In practice, however, one can treat a material as quasi-steady if its changes occur slowly compared with sampling times, and thereby recover the material evolution. Tseng et al. (2002a) developed fast methods to track the polymerization of F-actin. Additional examples include evolving rheology due to sudden chemical changes (Breedveld & Jan 2008, Sato & Breedveld 2006), polymerization (Slopek et al. 2006), gelation (Larsen & Furst 2008), and aging in nonergodic systems including glasses, gels, and foams (Bandyopadhyay et al. 2004, Bellour et al. 2003, Harden & Viasnoff 2001, Knaebel et al. 2000). For example, Jabbari-Farouji et al. 2007 established the validity of the FDT in a nonequilibrium glassy system through direct comparisons of thermally and actively driven probes in an aging colloidal glass.

4.2. How the Stokes Component Can Break Down

Whereas the Einstein component follows generally from equilibrium statistical mechanics—so that its failure reflects the breakdown of equilibrium in some way—the Stokes component requires a true hydrodynamic calculation, and its failure is more subtle, and potentially difficult to ascertain. In particular, the Stokes component reflects an inverse problem: Given a measured mobility in an unknown material, it gives the effective $G'(\omega)$ and $G''(\omega)$ that would be required to produce this mobility. Although apparent viscoelastic moduli can always be defined from measured diffusivity, such moduli may bear little resemblance to those measured macroscopically. To confidently recover macroscopic moduli from microrheology, it is crucial to understand when the Stokes component can be expected to hold. We have demonstrated its quantitative validity for any linear motion of a probe of any shape in any material that behaves as a homogeneous, isotropic, incompressible, quasi-steady, no-slip continuum (T.M. Squires & T.G. Mason, manuscript in preparation). Significantly, the failure of the Stokes component does not render microrheology worthless; instead, its proper interpretation can provide additional material information that would otherwise be inaccessible to macroscopic rheometry. We thus review a variety of ways in which the Stokes component can break down and new information and techniques that have been developed as a result.

4.2.1. Noncontinuum effects: probe size and material heterogeneity. An obvious assumption underlying the Stokes component is that the material behaves like a continuum, which requires length scales to be well separated. Material elements must exist that are large relative to the material's microstructure, so that they exhibit the same average response as a macroscopic material, yet must also be smaller than the relevant length scale for the flow around the probe (typically colloid radius). Soft materials often exhibit a wide variety of length scales—e.g., mesh spacing in gels, persistence length in semiflexible polymer solutions, or colloid and emulsion sizes—and these twin demands may be mutually incompatible.

Systematic microrheological studies have been performed using probes with a range of sizes and probe chemistries in simple Newtonian fluids (Valentine et al. 2001), un-cross-linked polymer solutions (Dasgupta et al. 2002, van Zanten et al. 2004), and in cross-linked polymer gels (Dasgupta & Weitz 2005), with consistent results for these materials. By contrast, Valentine et al. (2001) found that probes with radii of 1 μm or larger were effectively immobilized in an agarose gel, whereas submicrometer probes diffused freely, indicating micrometer-scale material porosity. Tuteja et al. (2007) measured nanoparticle diffusivity in entangled polymer melts to be orders of magnitude higher than the GSER would indicate, and reasoned that the nanoparticles are small enough to move through the melt without requiring entanglements to release, unlike the case for macroscale shear stresses.

Another example in which probe size matters is filamentous F-actin, a biopolymer that is particularly challenging owing to the range of relevant length scales, from submicrometer mesh lengths ξ to $\sim 10\text{-}\mu\text{m}$ persistence lengths, as well as differences in purification protocols. Probe size a can thus play a significant role: Free diffusion through actin networks is observed for nonadsorbing probes with $a \ll \xi$ (Gittes et al. 1997, McGrath et al. 2000, Schnurr et al. 1997, Valentine et al. 2004) and cage-hopping between transient pores when $a \sim \xi$ (Wong et al. 2004). The choice of probe size that would recover macroscopic viscoelasticity is also problematic: Probes that are larger than the persistence length would be non-Brownian. The scaling analysis of Maggs (1998), however, suggests that the geometric mean of the persistence and entanglement lengths is the relevant minimum probe size.

Finally, many complex fluids have been studied that exhibit material heterogeneities that are larger than microrheological probes, yet small enough to be effectively averaged in macroscopic rheometry. In such cases, microrheology can provide local information about the heterogeneous structure and rheology. Valentine et al. (2001) introduced a statistical framework for the interpretation of multiple particle-tracking techniques, which revealed the heterogeneous probe statistics within agarose gels to result from true porosity, rather than heterogeneous elasticity. By contrast, F-actin networks exhibited spatiotemporal heterogeneity, as confirmed by Wong et al. (2004). Using this framework, Dasgupta & Weitz (2005) showed that cross-linked poly-acrylamide gels exhibit heterogeneous elasticity.

Indeed, material heterogeneity provided a central motivation for two-point microrheology, discussed in Section 5.1, which uses cross-correlated probe motion to measure rheological properties that are effectively homogenized over longer (interprobe) length scales.

4.2.2. Anisotropic materials. Some materials exhibit equilibrium phases that are spatially homogeneous, yet also exhibit a preferred direction. For example, liquid crystalline materials are characterized by a director field that corresponds to local nematic order (see, e.g., de Gennes 1995, Stark 2001). Loudet and colleagues (2004) measured the anisotropic diffusivity of micrometer-scale oil droplets in a thermotropic nematic liquid crystal, which compared well with the Stokes drag calculations of Stark & Ventzki (2001). Because these experiments were performed in equilibrium, the Einstein component holds, and such agreement should be expected.

The Stokes component, conversely, need not be valid. The Erickson-Leslie equations for nematic liquid crystals are far more complicated than the Stokes equations for Newtonian fluids (see, e.g., Stark 2001), giving no reason to expect the GSM to yield a $G^*(\omega)$ that matches macroscopic rheometry. In fact, five distinct viscosities and (at least) four elastic constants are required to specify the constitutive relation, whereas only two distinct diffusivities (perpendicular and parallel to the local director field) are measured. One could define an effective viscosity from the diffusivity or mobility, as do Stark & Ventzki (2001), Loudet et al. (2004), and Lapointe et al. (2005); however, these quantities do not represent true material viscosities, but rather effective averages of the true parameters due to the complicated flow field around the probe. A quantitatively valid GSER for nematic liquid crystals would require the Leslie-Erickson equations to be solved for the frequency-dependent mobility of a given probe as a function of the various material parameters, probe-material anchoring conditions, and director orientation.

4.2.3. Probe-material interactions. Physical or chemical interactions between the probe and the material can alter the local material environment and cause the GSER to break down, even in materials that would otherwise seem ideal (e.g., homogeneous, isotropic, and continuum).

Physical interactions—e.g., depletion and electrostatic—can alter the local environment and affect diffusivity in a measurable way. For example, colloids embedded in solutions of semiflexible

polymers such as actin and DNA are surrounded by depletion zones of the order of the polymer correlation length (Morse 1998), as evidenced by the depletion forces they establish between colloids (Verma et al. 1998, 2000). Chen et al. (2003) used one- and two-point measurements to distinguish between local and material properties, and thus to ascertain features of the depleted region. In a seminal calculation, Levine & Lubensky (2000, 2001a) computed $M^*(\omega)$ for a spherical probe in a viscoelastic two-fluid material and modeled probe-material interactions by surrounding the probe with a thin spherical shell with different material constants. Indeed, they found the self-mobility $M^*(\omega)$ of a single probe to depend sensitively upon the local material environment. Moreover, they showed local heterogeneities to exert much less influence upon the correlated (coupling) mobility of two probes, giving a rigorous theoretical foundation for the two-point technique of Crocker et al. (2000), discussed below. Nagele (2003) used mode-coupling theory to demonstrate GSER violations in charge-stabilized colloidal suspensions, where repulsive probe-material interactions exclude suspension colloids from a region surrounding the probe. A particularly simple example was given by Squires (2008), who showed that the effective diffusivity of a probe surrounded by a depletion zone of relative thickness ε in a dilute colloidal suspension is $(1 - \varepsilon)^{-1}$ higher than the GSER would predict. Extensions to the theory of Levine & Lubensky (2000, 2001a) were carried out by Schmiedeberg & Stark (2005), who computed the analogous rotational mobility with the shell model, and Hill & Ostoja-Starzewski (2008), who expanded their treatment to include electrokinetic forcing.

Chemical interactions can also play a key role, for example, in coupling the probe to the elastic network. McGrath et al. (2000) found that probes whose chemistry was designed to prevent adsorption to F-actin networks were largely insensitive to the cross-link density of the network, and Valentine et al. (2004) found them to diffuse through the material as though it were water. By contrast, probes whose surface chemistry anchored the probe to the elastic network recovered their elastic properties. Schmiedeberg & Stark's (2005) theory showed that probe rotation was particularly sensitive to effective slip between the probe and the elastic phase, due to probe rotation without material deformation. By contrast, Dasgupta & Weitz (2005) measured the moduli of cross-linked poly-acrylamide gels (with $\xi \sim \text{nm}$) and found them to be independent of probe chemistry. In liquid crystalline materials, probe chemistry determines the local nematic order and introduces various topological defects (Stark 2001). Indeed, Koenig and colleagues (2009) measured nanoparticle diffusivities in nematic liquid crystals and found that they differ when the surface chemistry is varied to span the possible anchoring conditions.

4.2.4. Non-quasi-steady forcing. The GSM assumes fluid inertia to be negligible, which is not true for sufficiently high frequencies $\omega \geq \omega_I = \sqrt{|\eta^*(\omega)|/\rho a^2}$ [or equivalently $\omega_I \gtrsim |G^*(\omega)|/\rho a^2$]. At frequencies higher than ω_I , the oscillatory boundary layer or elastic wavelength ($\sim \sqrt{|\eta^*(\omega)|/\rho \omega}$) is smaller than the probe itself (Liverpool & MacKintosh 2005). Note the material inertia described here is distinct from that of the probe [$m\dot{V}(t)$ in Equation 8], and both must be negligible for the Stokes component to hold. Atakhorrami et al. (2005, 2008b) directly measured the cross-over from quasi-steady to inertial in the coupling mobility between two probes, and found excellent agreement with the computed flows of Liverpool & MacKintosh (2005) and Oseen (1927). The quasi-steady requirement imposes a stronger frequency constraint on macroscopic shear rheology, for which the gap spacing b replaces the probe size a in setting ω_I . Microrheology can thus directly probe significantly higher frequencies, without requiring time-temperature superposition (e.g., Bird et al. 1987).

4.2.5. Osmotic compressibility. Whereas the viscous solvent in complex fluids is almost always incompressible, elastic components are often not (i.e., Poisson ratio $\nu \neq 1/2$). Suspended

structures are generally compressed in front of a forced probe and dilated behind, driving osmotic compression within an incompressible solvent. Indeed, the displacement of a sphere in a compressible elastic medium under a steady force F is given by

$$\Delta x = \frac{1}{6\pi G'a} \left(1 + \frac{2\nu - 1}{4(\nu - 1)} \right) F. \quad (26)$$

To achieve this steady-state compression, however, solvent must flow from front to rear through the elastic structure. Gittes et al. (1997) and Schnurr et al. (1997) argue that this drainage time in polymer gels occurs when local elastic compressional forces $f_e \sim G'\nabla^2 u \sim \eta''u/a^2$ balance viscous draining forces $f_v \sim \eta\nabla^2 v \sim \eta\omega u/\xi^2$, where ξ is the characteristic mesh size. The elastic network deforms affinely with the flow for frequencies above $\omega_c \sim G'\xi^2/\eta a^2$ because the fluid is unable to flow quickly enough to accommodate compression and dilation. At lower frequencies, by contrast, the elastic and fluid phases effectively decouple and freely drain, causing quantitative discrepancies between the GSER and microrheology. For Gittes et al.'s (1997) F-actin measurements, for example, $\omega_c \sim 10$ Hz, leaving approximately five decades of frequency where the GSER is expected to hold. Detailed calculations (Levine & Lubensky 2000, 2001a) support these scaling arguments. Hill & Ostoja-Starzewski (2008) argued that the relatively short drainage time around a micrometer-scale probe, compared with that in a large sample, enables more sensitive measurements of compressibility with microrheology than macroscopic techniques. Osmotic compressibility also affects the microrheology of colloidal suspensions: Probe-suspension collisions statistically increase the concentration in front of the probe and decrease it behind. For this compressed region to form, suspension particles must have time to diffuse across the probe (Khair & Brady 2005, Sriram et al. 2009).

5. EXTENSIONS AND FUTURE WORK

The above discussion highlights the reasons for the remarkably general success that microrheology has enjoyed: As long as the probe is inert and the material behaves as a quasi-steady, near-equilibrium, homogeneous, isotropic, and incompressible continuum, the GSER will faithfully and quantitatively recover the frequency-dependent viscoelastic moduli typically measured in a conventional rheometer. In what follows, we discuss two cases in which the basic technique has been expanded in response to systems where these assumptions are not valid.

5.1. Multiparticle Microrheology

Tracking multiple probes in microrheology can be advantageous for a variety of reasons. For example, long-time convective drift is often the major source of disagreement between particle-tracking microrheology and macroscopic rheology, and eliminating correlated motion provides an effective strategy to obtain the correct low-frequency behavior. To do so, Mason et al. (1997a) tracked the trajectories of two nearby fluorescent probe spheres in concentrated DNA solutions, and subtracted their collective motion to remove stray convective drift from probe trajectories, thus enabling measurements of probe self-diffusivities over longer times.

Multiparticle techniques are also advantageous in investigations of heterogeneous materials. The statistics of individually tracked particles encode information about the local environment around each; such information is completely inaccessible to macroscopic rheometry and is lost in, e.g., light-scattering techniques, which ensemble-average the statistics of many probes. Apgar et al. (2000), Tseng and colleagues (2002a,b; Tseng & Wirtz 2001), and Xu et al. (1998a,b) used multiparticle techniques in their studies of biopolymer networks and living cells (reviewed in Wirtz 2009). Crocker et al. (2000), Valentine et al. (2001), and Dasgupta and colleagues (2002;

Dasgupta & Weitz 2005) tracked $\sim 10^2$ probes simultaneously in both simple and complex materials.

With additional statistics comes the need to interpret them meaningfully. Valentine et al. (2001) introduced van Hove correlation plots and F-statistics to determine when heterogeneous single-probe behavior indicated heterogeneous material properties. Murray & Grier (1996) and Crocker & Grier (1996) developed widely used particle-tracking techniques for such measurements, for which errors due to statistics, sampling, and noise discrimination were carefully studied and minimized by Savin and colleagues (2008; Savin & Doyle 2005, 2007).

Many soft materials are fundamentally inhomogeneous, and additionally may interact physically and chemically with the probe, potentially causing the GSER to fail. To address such limitations, Crocker et al. (2000) introduced two-point microrheology, for which Levine & Lubensky (2000, 2001a,b) provided the theoretical framework. The key insight behind two-point microrheology is that the hydrodynamic interactions between two probes are mediated through the material between the particles, so that the complex viscosity $\tilde{\eta}(s)$ that they encode is more sensitive to the bulk material rheology than (one-point) self-mobility measurements.

In two-point microrheology, hydrodynamic interactions are measured via the cross-correlation of two distinct probe positions. The FDT relates these cross-correlations to the coupling mobility M_{12} ,

$$\mathcal{L}(\Delta x_1(0)\Delta x_2(t)) \equiv \frac{2k_B T}{s^2} \tilde{M}_{12}(s), \quad (27)$$

which is an off-diagonal component (or block) of the grand multiparticle mobility tensor relating the velocity V_1 of particle 1 in response to a force F_2 on particle 2 (see Batchelor 1976). (Note that the coupling mobility is not an eigenmode of the multiparticle mobility, and is thus not the inverse of the coupling resistance.) The Oseen tensor gives the leading-order approximation to the Newtonian coupling mobility M_{12} for well-separated probes, with parallel (\parallel) and perpendicular (\perp) components given by $M_{12}^{\parallel} \sim (4\pi\eta d)^{-1}$ and $M_{12}^{\perp} \sim (8\pi\eta d)^{-1}$, where d is the interprobe distance. The (far-field) coupling mobility does not depend on the size (or shape) of either probe, further emphasizing the dominant role played by the medium between the probes, rather than the environment around each. Levine & Lubensky (2000, 2001a) computed one- and two-point mobilities for probes in a two-fluid model LVE material, with each probe surrounded by a shell with different viscoelastic properties. Indeed, they found the coupling mobility to be far less sensitive to the shell than the one-point (self-)mobility.

Levine & Lubensky (2001b) developed an electrostatic analogy to give an intuitive sense for the coupling mobility and two-point microrheology. An entirely equivalent analogy in heat transfer (likely more familiar to the fluids community) was suggested by A.S. Khair (personal communication). The (one-point) temperature T_1 of a sphere to which a heat flux Q_1 is forced depends sensitively upon the properties of any insulating shell around that sphere. The (two-point) temperature T_2 of a well-separated second sphere in response to the heat flux Q_1 emanating from the first sphere, however, depends more strongly on the medium between the spheres than upon T_1 . The analogy with two-point microrheology follows with T corresponding to \mathbf{v} , Q to \mathbf{F} , and thermal conductivity to η .

Using multiple-particle tracking, Crocker et al. (2000) compared one- and two-point measurements of heterogeneous materials, finding two-point techniques to more faithfully recover the macroscopic rheology of guar gum and suggesting that one-point measurements of F-actin should be re-examined. Valentine et al. (2004) showed that two-point measurements were insensitive to probe chemistry, whereas one-point methods can be insensitive for certain probes and materials. The comparison between one- and two-point measurements in multiparticle-tracking experiments can be used to provide complementary information about material. Examples

include measuring the depletion layer local to each probe in DNA solutions (Chen et al. 2003), elucidating distinct contributions to the elasticity of F-actin (Gardel et al. 2003), measuring length-scale-dependent rheology (Liu et al. 2006), arguing for probe/polymer slip in polymer solutions (Starrs & Bartlett 2003), and identifying heterogeneity and ATP dependence in living cells (Hoffman et al. 2006). Heterogeneities with length scales larger than the interprobe separations, conversely, would not be averaged.

Two-point microrheology requires the collection and analysis of much more data to obtain sufficient statistics than one-point microrheology, because the coupling mobility M_{12} is generally $\mathcal{O}(a/d)$ weaker than the self-mobility M_{11} . This can make two-point techniques significantly more difficult to implement. Starrs & Bartlett (2003) used dual optical traps to hold probe pairs at specified separations in a polymer solution, thus improving the statistics and frequency range at each. Buchanan et al. (2005) and Atakhorrami et al. (2006) carefully compared one- and two-point microrheology with macroscopic rheometry of wormlike micellar solutions, finding excellent agreement at all frequency ranges. In high-frequency two-point experiments of the moduli of F-actin, Koenderink et al. (2006) measured the compressibility of the elastic phase through its dependence on $M_{12}^{\perp}/M_{12}^{\parallel}$ (Levine & Lubensky 2001a). Actively driving one probe (e.g., with a laser tweezer) and measuring the response of the other can improve the magnitude of the response (Atakhorrami et al. 2008a, Hough & Ou-Yang 2002). Atakhorrami et al. (2008a) described dual-optical-trap experiments, which give rise to additional complications, including position anticorrelations due to hydrodynamic interactions during relaxation (Atakhorrami et al. 2006, Meiners & Quake 1999), and the reduced ω_I at which quasi-steadiness breaks down because of the increased (interprobe) distance required for vorticity propagation (Atakhorrami et al. 2005, 2008b; Liverpool & MacKintosh 2005).

5.2. Active and Nonlinear Microrheology

The equilibrium nature of passive microrheological measurements ensures that linear visco-elastic moduli are measured. The nonlinear rheological response of a material, however, is often equally important for material processing, performance, and understanding (Bird et al. 1987, Larson 1999). For example, yield stresses allow frosting to be spread, yet keep it on the side of a cake. Normal stress effects cause viscoelastic materials to swell when extruded and to climb stirrers during mixing. Shear-thinning materials are frequently used as lubricants, and shear-thickening materials can lead to sudden equipment failure.

These nonlinear rheological phenomena arise because of microstructures that are driven significantly out of equilibrium and are thus inaccessible to equilibrium passive microrheology. The advantages of microrheology—e.g., small sample volumes, local probes of material heterogeneity—provide significant motivation to develop microrheological techniques capable of extracting these nonlinear response properties. Pipe & McKinley (2009) review recent microfluidic strategies for doing so; here we focus on probe-based techniques.

In active and nonlinear microrheology, a probe is actively forced within the material, with the hopes of driving the material out of equilibrium and measuring a rheologically meaningful nonlinear response. In essence, active and nonlinear microrheology is a microversion of falling-ball or towed-ball viscometry, in which a steady drag mobility $M(V)$ is interpreted—often using a GSM—to recover the rate-dependent viscosity. Unlike shear rheology, however, falling-ball viscometry is generally viewed as providing an index for viscosity, rather than a quantitative measurement (Macosko 1994).

A variety of researchers have actively driven probes to measure their nonlinear response in the material. Magnetic forces have been used to force beads through colloidal suspensions near the

glass transition (Habdas et al. 2004) and nanowires through wormlike micellar solutions (Cappallo et al. 2007). Colloidal probes have been forced using laser tweezers through colloidal fluids (Meyer et al. 2006, Wilson et al. 2009) and DNA solutions (Gutsche et al. 2008), with simultaneous measurements of the nonequilibrium microstructure around the probe. Gravity can also be used as an external force: Verhoeff and colleagues (2008) measured the sedimentation of 10- μm silica probes through a colloidal liquid crystal to recover an orientation-dependent Stokes drag that disagreed even qualitatively with the (linear-response) theory of Stark & Venzki (2001), presumably due to the nonlinear response at significant Erickson numbers (Stark & Venzki 2002). Wilking & Mason (2008) optically torqued wax microdisks to measure local yielding of gelatin.

Because nonlinear microrheology probes the response of a material driven out of equilibrium, the linear-response machinery used to derive the GSER and justify its generality is not valid. It is thus not clear how to interpret the experiments in a rheologically meaningful way. Although one might hope that a simple velocity-dependent GSM might hold, there is no theoretical reason to expect it will do so in general. The very comparison between a velocity-dependent viscosity $\eta(V)$ (obtained assuming the GSM to hold) and a shear-rate dependent $\eta(\dot{\gamma})$ is problematic, as a range of strain rates exists around the driven probe. More quantitative comparisons can be made by identifying dimensionless numbers appropriate for the material microstructure (e.g., the Peclet number for colloidal suspensions and the Erickson number for liquid crystals), although the multiple length scales inherent to such systems make this choice ambiguous (Squires 2008).

To determine the nonlinear probe response (i.e., the nonlinear version of the Stokes component), the perturbed microstructure must generally be computed explicitly. Initial theoretical work in nonlinear microrheology focused on dilute colloidal suspensions, which represent perhaps the simplest materials whose microstructure can be explicitly computed. In particular, perturbations due to direct collisions between the probe and suspended particles were the initial focus (Gutsche et al. 2008, Khair & Brady 2006, 2007, 2008; Squires & Brady 2005). The computed microstructures resembled experimental measurements (Gutsche et al. 2008, Meyer et al. 2006), and scaled features of the computed mobility agreed with analogous theory (Bergenholtz et al. 2002), Brownian dynamics simulations (Carpen & Brady 2005), and some features of experiments (Meyer et al. 2006). Subsequently, however, Squires (2008) argued that these direct probe-material interactions have no analog in macroscopic rheology, because rheometer plates do not collide with the material, and that bulk stresses were more pertinent.

Motivated by the common limit shared by passive and active microrheology,

$$\lim_{\omega \rightarrow 0} M^*(\omega) = \lim_{V \rightarrow 0} M(V), \quad (28)$$

Sriram et al. (2009) sought to bridge the two, by using the theoretical machinery developed for the nonlinear microrheology of suspensions (Khair & Brady 2006, Squires & Brady 2005, Squires 2008) to explicitly compute the microstructural deformations in a linear microrheology system. Although the FDT renders such explicit computations unnecessary, these calculations explicitly connect features in the nonlinear problem with their analogs in linear systems. For example, the microstructure induced by direct probe-material collisions (Gutsche et al. 2008; Khair & Brady 2006, 2007, 2008; Squires & Brady 2005) represents the steady-drag analog of osmotic compressibility effects (Gittes et al. 1997, Schnurr et al. 1997). Indeed, Sriram et al. (2009) found quantitative agreement between theory and experiment only for microstructural deformations within the bulk material, rather than for direct probe-material interactions.

More generally, Squires (2008) identified and discussed key challenges that complicate the interpretation of nonlinear microrheology. (a) The flow around the probe is not viscometric (pure shear), as it is in macroscopic shear rheology. Extensional viscosities can differ from shear

viscosities by orders of magnitude (Bird et al. 1987), and nonlinear microrheology naturally gives rise to a range of mixed flows around the probe. Similar complications exist for the multiple viscosities exhibited by liquid crystalline materials (Stark 2001). (b) Material elements do not respond instantaneously to the local deformation field $\dot{\epsilon}(t)$, but exhibit a transient stress response. The Lagrangian unsteadiness experienced by material elements as they advect around the probe may prevent the stress field from achieving a steady nonlinear response. (c) Finally, the rate of deformation tensor $\dot{\epsilon}(t)$ is spatially inhomogeneous even for simple Stokes flows around the probe. (By contrast, small-amplitude oscillatory forcing deforms the surrounding material at a single frequency.) Even if a material would respond quasi-steadily to the local strain rate, the probe mobility would reflect a weighted average of various states of stress. Squires (2008) showed the mobility to be invertible in a simple model material under extremely limited conditions, quantitatively recovering $\eta(\dot{\epsilon})$ from $M(V)$. Squires (2008) also suggested geometric modifications: Forced needle-like probes establish a more nearly pure shear flow and steady strain rate along the length of the needle, and may reproduce nonlinear rheology more faithfully.

6. DISCUSSION AND CONCLUSIONS

Microrheology links observations of the motion of probe colloids in soft materials to the mechanical properties of those materials. In many cases, broadband thermal fluctuations cause probe excitations that can be interpreted using thermal diffusion microrheology. Active approaches for exciting the probes provide alternatives for obtaining both linear and nonlinear local rheological properties. To obtain meaningful results from any microrheological technique, one must be discerning in choosing among the many different techniques and their implementation. We have reviewed many of these considerations, which include the probe size and shape relative to structures that give rise to the non-Newtonian behavior of the soft material, the type of binding of the probe to the material, and material inhomogeneities and anisotropies.

In addition, this review provides a theoretical and analytical summary of the field of microrheology at present. As the field has emerged, several different preferences for analytical approaches, each with its own notation, have been used to characterize and report thermal diffusion microrheology results. These seemingly different approaches are equivalent, and reflect energy equipartition, causality, and the FDT. We examine the assumptions and approximations inherent in both the Stokes and Einstein components of the GSER, which must be understood to properly measure the microrheology of specific types of soft materials.

SUMMARY POINTS

1. The linear mechanical response of soft materials to weak forces is generally frequency dependent and viscoelastic, and is described by a complex shear modulus $G^*(\omega) = G'(\omega) + iG''(\omega)$, which encodes information about the equilibrium microstructure and dynamics of the material.
2. Microrheology uses micrometer-scale probes embedded within materials to measure local and bulk rheological properties, such as $M^*(\omega)$ and $G^*(\omega)$. Probes can be driven actively by an externally applied force, or passively, by thermal fluctuations in the material.
3. Any method for measuring the mean square displacement of embedded probes can potentially be used for passive microrheology, including methods that ensemble-average the response of probes within a given volume (e.g., light scattering or NMR), as well as the direct tracking of individual particles.

4. The quantity measured in probe-based microrheology is the mobility of the probe within the material, from which the material rheology is extracted using a generalized Stokes-Einstein relation (GSER) whose validity is generally assumed. The GSER, similar to the linear viscoelastic moduli, can be represented in a variety of completely equivalent ways.
5. The Einstein component of the GSER requires the probe and material to be in equilibrium, and can break down in systems in which the probe is actively forced, or the material is itself active or evolving.
6. The Stokes component of the GSER relates the measured mobility of the probe to the complex shear modulus of the material. Its validity requires the surrounding material to behave as a homogeneous, isotropic, quasi-steady, incompressible continuum.
7. The cross-correlated (two-point) response of multiple probes is sensitive to the properties of the material between the probes, whereas individual probes respond more to the local environment. In heterogeneous materials, two-point techniques recover the macroscopic shear rheology more faithfully than single-point measurements, and the combination of the two techniques provides complementary information about the material.
8. Actively forced probes can be used to drive a material out of equilibrium, with the goal of extracting information about the nonlinear rheological response of a material from the velocity-dependent mobility. A number of complications arise, and open challenges remain, in the proper interpretation of nonlinear mobility measurements in terms of nonlinear rheology.

DISCLOSURE STATEMENT

The authors are not aware of any affiliations, memberships, funding, or financial holdings that might be perceived as affecting the objectivity of this review.

ACKNOWLEDGMENTS

T.M.S. gratefully acknowledges support of NSF under CBET-0730270 for this work.

LITERATURE CITED

- Amblard F, Maggs AC, Yurke B, Pargellis AN, Leibler S. 1996. Subdiffusion and anomalous local viscoelasticity in actin networks. *Phys. Rev. Lett.* 77:4470–73
- Apgar J, Tseng Y, Fedorov E, Herwig MB, Almo SC, Wirtz D. 2000. Multiple-particle tracking measurements of heterogeneities in solutions of actin filaments and actin bundles. *Biophys. J.* 79:1095–106
- Atakhorrami M, Koenderink GH, Schmidt CF, MacKintosh FC. 2005. Short-time inertial response of viscoelastic fluids: observation of vortex propagation. *Phys. Rev. Lett.* 95:208302
- Atakhorrami M, Addas KM, Schmidt CF. 2008a. Twin optical traps for two-particle cross-correlation measurements: eliminating cross-talk. *Rev. Sci. Instrum.* 79:043103
- Atakhorrami M, Mizuno D, Koenderink GH, Liverpool TB, MacKintosh FC, Schmidt CF. 2008b. Short-time inertial response of viscoelastic fluids measured with Brownian motion and with active probes. *Phys. Rev. E* 77:061508
- Atakhorrami M, Schmidt CF. 2006. High-bandwidth one- and two-particle microrheology in solutions of wormlike micelles. *Rheol. Acta* 45:449–56

This work introduces a rotational form of the GSER and shows that rotational tracking of thermally excited particles can be used to obtain linear viscoelasticity.

First experimental demonstration of two-point microrheology.

- Atakhorrami M, Sulkowska JI, Addas KM, Koenderink GH, Tang JX, et al. 2006. Correlated fluctuations of microparticles in viscoelastic solutions: quantitative measurement of material properties by microrheology in the presence of optical traps. *Phys. Rev. E* 73:061501
- Bandyopadhyay R, Liang D, Yardimci H, Sessoms DA, Borthwick MA, et al. 2004. Evolution of particle-scale dynamics in an aging clay suspension. *Phys. Rev. Lett.* 93:228302
- Batchelor GK. 1976. Brownian diffusion of particles with hydrodynamic interaction. *J. Fluid Mech.* 74:1–29
- Bausch AR, Ziemann F, Boulbitch AA, Jacobson K, Sackmann E. 1998. Local measurements of viscoelastic parameters of adherent cell surfaces by magnetic bead microrheometry. *Biophys. J.* 75:2038–49
- Bellour M, Knaebel A, Harden JL, Lequeux F, Munch JP. 2003. Aging processes and scale dependence in soft glassy colloidal suspensions. *Phys. Rev. E* 67:031405
- Bergenholtz J, Brady JF, Vico M. 2002. The non-Newtonian rheology of dilute colloidal suspensions. *J. Fluid Mech.* 456:239–75
- Berne BJ, Pecora R. 2000. *Dynamic Light Scattering: With Applications to Chemistry, Biology, and Physics*. New York: Dover
- Bird RB, Armstrong RC, Hassager O. 1987. *Dynamics of Polymeric Liquids*, Vol. 1: *Fluid Mechanics*. New York: Wiley & Sons
- Bishop AI, Nieminen TA, Heckenberg NR, Rubinsztein-Dunlop H. 2004. Optical microrheology using rotating laser-trapped particles. *Phys. Rev. Lett.* 92:198104
- Breedveld V, Jan JS. 2008. Microrheological study of polyelectrolyte collapse and reexpansion in the presence of multivalent counterions. *Macromolecules* 41:6517–22
- Breedveld V, Pine DJ. 2003. Microrheology as a tool for high-throughput screening. *J. Mater. Sci.* 38:4461–70
- Brunner C, Niendorf A, Kas JA. 2009. Passive and active single-cell biomechanics: a new perspective in cancer diagnosis. *Soft Matter* 5:2171–78
- Buchanan M, Atakhorrami M, Palierne JF, Schmidt CF. 2005. Comparing macrorheology and one- and two-point microrheology in wormlike micelle solutions. *Macromolecules* 38:8840–44
- Cappallo N, Lapointe C, Reich DH, Leheny RL. 2007. Nonlinear microrheology of wormlike micelle solutions using ferromagnetic nanowire probes. *Phys. Rev. E* 76:031505
- Cardinaux F, Cipelletti L, Scheffold F, Schurtenberger P. 2002. Microrheology of giant-micelle solutions. *Europhys. Lett.* 57:738–44
- Carpen IC, Brady JF. 2005. Microrheology of colloidal dispersions by Brownian dynamics simulations. *J. Rheol.* 49:1483–502
- Chen DT, Weeks ER, Crocker JC, Islam MF, Verma R, et al. 2003. Rheological microscopy: local mechanical properties from microrheology. *Phys. Rev. Lett.* 90:108301
- Cheng Z, Mason TG. 2003. Rotational diffusion microrheology. *Phys. Rev. Lett.* 90:018304**
- Crick FHC, Hughes AFW. 1950. The physical properties of cytoplasm: a study by means of the magnetic particle method. 1. Experimental. *Exp. Cell Res.* 1:37–80
- Crocker JC, Grier DG. 1996. Methods of digital video microscopy for colloidal studies. *J. Colloid Interface Sci.* 179:298–310
- Crocker JC, Valentine MT, Weeks ER, Gisler T, Kaplan PD, et al. 2000. Two-point microrheology of inhomogeneous soft materials. *Phys. Rev. Lett.* 85:888–91**
- Dasgupta BR, Tee SY, Crocker JC, Frisken BJ, Weitz DA. 2002. Microrheology of polyethylene oxide using diffusing wave spectroscopy and single scattering. *Phys. Rev. E* 65:051505
- Dasgupta BR, Weitz DA. 2005. Microrheology of cross-linked polyacrylamide networks. *Phys. Rev. E* 71:021504
- de Gennes PG. 1995. *The Physics of Liquid Crystals*. Oxford: Oxford Univ. Press
- Edwards DA, Brenner H, Wasan DT. 1991. *Interfacial Transport Processes and Rheology*. Boston: Butterworth-Heinemann
- Einstein A. 1905. Über die von der molekularkinetischen Theorie der Wärme geforderte Bewegung von in ruhenden Flüssigkeiten suspendierten Teilchen. *Ann. Phys. (Leipzig)* 17:549–60
- Evans RML, Tassieri M, Auhl D, Waigh TA. 2009. Direct conversion of rheological compliance measurements into storage and loss moduli. *Phys. Rev. E* 80:012501
- Fischer TM. 2004. Comment on “Shear viscosity of Langmuir monolayers in the low-density limit”. *Phys. Rev. Lett.* 92:139603

- Fletcher DA, Geissler PL. 2009. Active biological materials. *Annu. Rev. Phys. Chem.* 60:469–86
- Freundlich H, Seifriz W. 1922. Ueber die Elastizitat von Solen und Gelen. *Z. Phys. Chem.* 104:233
- Furst EM. 2005. Applications of laser tweezers in complex fluid rheology. *Curr. Opin. Colloid Interface Sci.* 10:79–86
- Gallet F, Arcizet D, Bohec P, Richert A. 2009. Power spectrum of out-of-equilibrium forces in living cells: amplitude and frequency dependence. *Soft Matter* 5:2947–53
- Gardel ML, Valentine MT, Crocker JC, Bausch AR, Weitz DA. 2003. Microrheology of entangled F-actin solutions. *Phys. Rev. Lett.* 91:158302
- Gardel ML, Weitz DA. 2005. Microrheology. In *Microscale Diagnostic Techniques*, ed. KS Breuer, pp. 1–50. Berlin: Springer
- Gisler T, Weitz DA. 1998. Tracer microrheology in complex fluids. *Curr. Opin. Colloid Interface Sci.* 3:586–92
- Gisler T, Weitz DA. 1999. Scaling of the microrheology of semidilute F-actin solutions. *Phys. Rev. Lett.* 82:1606–9
- Gittes F, Schnurr B, Olmsted PD, MacKintosh FC, Schmidt CF. 1997. Microscopic viscoelasticity: shear moduli of soft materials determined from thermal fluctuations. *Phys. Rev. Lett.* 79:3286–89
- Gutsche C, Kremer F, Kruger M, Rauscher M, Weeber R, Harting J. 2008. Colloids dragged through a polymer solution: experiment, theory, and simulation. *J. Chem. Phys.* 129:084902
- Habdas P, Schaar D, Levitt AC, Weeks ER. 2004. Forced motion of a probe particle near the colloidal glass transition. *Europhys. Lett.* 67:477–83
- Harden JL, Viasnoff V. 2001. Recent advances in DWS-based micro-rheology. *Curr. Opin. Colloid Interface Sci.* 6:438–45
- Heilbronn A. 1922. Eine neue Methode zur Bestimmung der Viskositat lebender Protoplasten. *Jabrb. Wiss. Bot.* 61:284–338
- Henle ML, McGorty R, Schofield AB, Dinsmore AD, Levine AJ. 2008. The effect of curvature and topology on membrane hydrodynamics. *Europhys. Lett.* 84:48001
- Hill RJ, Ostoja-Starzewski M. 2008. Electric-field-induced displacement of a charged spherical colloid embedded in an elastic Brinkman medium. *Phys. Rev. E* 77:011404
- Hoffman BD, Massiera G, Van Citters KM, Crocker JC. 2006. The consensus mechanics of cultured mammalian cells. *Proc. Natl. Acad. Sci. USA* 103:10259–64**
- Hough LA, Ou-Yang HD. 2002. Correlated motions of two hydrodynamically coupled particles confined in separate quadratic potential wells. *Phys. Rev. E* 65:021906
- Jabbari-Farouji S, Mizuno D, Atakhorrami M, MacKintosh FC, Schmidt CF, et al. 2007. Fluctuation-dissipation theorem in an aging colloidal glass. *Phys. Rev. Lett.* 98:108302
- Khair AS, Brady JF. 2005. “Microviscoelasticity” of colloidal dispersions. *J. Rheol.* 49:1449–81
- Khair AS, Brady JF. 2006. Single particle motion in colloidal dispersions: a simple model for active and nonlinear microrheology. *J. Fluid Mech.* 557:73–117
- Khair AS, Brady JF. 2007. On the motion of two particles translating with equal velocities through a colloidal dispersion. *Proc. R. Soc. A* 463:223–40
- Khair AS, Brady JF. 2008. Microrheology of colloidal dispersions: shape matters. *J. Rheol.* 52:165–96
- Knaebel A, Bellour M, Munch JP, Viasnoff V, Lequeux F, Harden JL. 2000. Aging behavior of laponite clay particle suspensions. *Europhys. Lett.* 52:73–79
- Koenderink GH, Atakhorrami M, MacKintosh FC, Schmidt CF. 2006. High-frequency stress relaxation in semiflexible polymer solutions and networks. *Phys. Rev. Lett.* 96:138307
- Koenig GM, Ong R, Cortes AD, Moreno-Razo JA, de Pablo JJ, Abbott NL. 2009. Single nanoparticle tracking reveals influence of chemical functionality of nanoparticles on local ordering of liquid crystals and nanoparticle diffusion coefficients. *Nano Lett.* 9:2794–801
- Kuo SC, Sheetz MP. 1993. Force of single kinesin molecules measured with optical tweezers. *Science* 260:232–34
- Landau LD, Lifshitz EM. 2000. *Statistical Physics*. Oxford: Butterworth-Heinemann
- Lapointe C, Cappallo N, Reich DH, Leheny RL. 2005. Static and dynamic properties of magnetic nanowires in nematic fluids. *J. Appl. Phys.* 97:10Q304
- Larsen TH, Furst EM. 2008. Microrheology of the liquid-solid transition during gelation. *Phys. Rev. Lett.* 100:146001

Uses four separate microrheological methods, including active and passive, one- and two-point techniques, to measure rotational and translational motion of probes in cultured mammalian cells, with and without ATP.

This theoretical foundation (and later related work by the same authors) extends classic single-particle microrheology to two-point microrheology.

Concurrent with Schnurr et al. 1997, introduces a real-space particle-tracking method and applies the GSER to measure thermal microrheology of soft materials using laser-deflection particle tracking.

Founding presentation of thermal (i.e., passive) microrheology of soft materials, and initial validation of the GSER.

- Larson RG. 1999. *The Structure and Rheology of Complex Fluids*. New York: Oxford Univ. Press
- Levine AJ, Lubensky TC. 2000. One- and two-particle microrheology. *Phys. Rev. Lett.* 85:1774–77**
- Levine AJ, Lubensky TC. 2001a. Response function of a sphere in a viscoelastic two-fluid medium. *Phys. Rev. E* 63:041510
- Levine AJ, Lubensky TC. 2001b. Two-point microrheology and the electrostatic analogy. *Phys. Rev. E* 65:011501
- Liu J, Gardel ML, Kroy K, Frey E, Hoffman BD, et al. 2006. Microrheology probes length scale dependent rheology. *Phys. Rev. Lett.* 96:118104
- Liverpool TB, MacKintosh FC. 2005. Inertial effects in the response of viscous and viscoelastic fluids. *Phys. Rev. Lett.* 95:208303
- Liverpool TB, Maggs AC, Ajdari A. 2001. Viscoelasticity of solutions of motile polymers. *Phys. Rev. Lett.* 86:4171–74
- Loudet JC, Hanusse P, Poulin P. 2004. Stokes drag on a sphere in a nematic liquid crystal. *Science* 306:1525
- Lugowski R, Kolodziejczyk B, Kawata Y. 2002. Application of laser-trapping technique for measuring the three-dimensional distribution of viscosity. *Opt. Commun.* 202:1–8
- MacKintosh FC, Levine AJ. 2008. Nonequilibrium mechanics and dynamics of motor-activated gels. *Phys. Rev. Lett.* 100:018104
- MacKintosh FC, Schmidt CF. 1999. Microrheology. *Curr. Opin. Colloid Interface Sci.* 4:300–7
- Macosko CW. 1994. *Rheology: Principles, Measurements, and Applications*. New York: Wiley & Sons
- Maggs AC. 1998. Micro-bead mechanics with actin filaments. *Phys. Rev. E* 57:2091–94
- Martin P, Hudspeth AJ, Julicher F. 2001. Comparison of a hair bundle's spontaneous oscillations with its response to mechanical stimulation reveals the underlying active process. *Proc. Natl. Acad. Sci. USA* 98:14380–85
- Mason TG. 2000. Estimating the viscoelastic moduli of complex fluids using the generalized Stokes-Einstein equation. *Rheol. Acta* 39:371–78
- Mason TG, Dhople A, Wirtz D. 1997a. Concentrated DNA rheology and microrheology. *Mater. Res. Soc. Symp. Proc.* 463:153–58
- Mason TG, Ganesan K, van Zanten JH, Wirtz D, Kuo SC. 1997b. Particle tracking microrheology of complex fluids. *Phys. Rev. Lett.* 79:3282–85**
- Mason TG, Gang H, Weitz DA. 1996. Rheology of complex fluids measured by dynamic light scattering. *J. Mol. Struct.* 383:81–90
- Mason TG, Gang H, Weitz DA. 1997c. Diffusing-wave-spectroscopy measurements of viscoelasticity of complex fluids. *J. Opt. Soc. Am. A* 14:139–49
- Mason TG, Weitz DA. 1995. Optical measurements of frequency-dependent linear viscoelastic moduli of complex fluids. *Phys. Rev. Lett.* 74:1250–53**
- McGrath JL, Hartwig JH, Kuo SC. 2000. The mechanics of F-actin microenvironments depend on the chemistry of probing surfaces. *Biophys. J.* 79:3258–66
- Meiners JC, Quake SR. 1999. Direct measurement of hydrodynamic cross correlations between two particles in an external potential. *Phys. Rev. Lett.* 82:2211–14
- Meyer A, Marshall A, Bush BG, Furst EM. 2006. Laser tweezer microrheology of a colloidal suspension. *J. Rheol.* 50:77–92
- Mizuno D, Head DA, MacKintosh FC, Schmidt CF. 2008. Active and passive microrheology in equilibrium and nonequilibrium systems. *Macromolecules* 41:7194–7202
- Mizuno D, Tardin C, Schmidt CF, MacKintosh FC. 2007. Nonequilibrium mechanics of active cytoskeletal networks. *Science* 315:370–73
- Morse DC. 1998. Viscoelasticity of concentrated isotropic solutions of semiflexible polymers. 2. Linear response. *Macromolecules* 31:7044–67
- Murray CA, Grier DG. 1996. Video microscopy of monodisperse colloidal systems. *Annu. Rev. Phys. Chem.* 47:421–62
- Nagele G. 2003. Viscoelasticity and diffusional properties of colloidal model dispersions. *J. Phys. Condens. Matter* 15:S407–14
- Nedelec FJ, Surrey T, Maggs AC, Leibler S. 1997. Self-organization of microtubules and motors. *Nature* 389:305–8

- Oseen CW. 1927. *Hydrodynamik*. Leipzig: Akad. Verlagsgesellschaft
- Pipe CJ, McKinley GH. 2009. Microfluidic rheometry. *Mech. Res. Commun.* 36:110–20
- Prasad V, Weeks ER. 2009. Two-dimensional to three-dimensional transition in soap films demonstrated by microrheology. *Phys. Rev. Lett.* 102:178302
- Reif F. 1965. *Fundamentals of Statistical and Thermal Physics*. New York: McGraw-Hill
- Saffman PG, Delbruck M. 1975. Brownian motion in biological membranes. *Proc. Natl. Acad. Sci. USA* 72:3111–13
- Sato J, Breedveld V. 2006. Transient rheology of solvent-responsive complex fluids by integrating microrheology and microfluidics. *J. Rheol.* 50:1–19
- Savin T, Doyle PS. 2005. Static and dynamic errors in particle tracking microrheology. *Biophys. J.* 88:623–38
- Savin T, Doyle PS. 2007. Statistical and sampling issues when using multiple particle tracking. *Phys. Rev. E* 76:021501
- Savin T, Spicer PT, Doyle PS. 2008. A rational approach to noise discrimination in video microscopy particle tracking. *Appl. Phys. Lett.* 93:024102
- Schmidt FG, Hinner B, Sackmann E. 2000. Microrheometry underestimates the values of the viscoelastic moduli in measurements on F-actin solutions compared to macrorheometry. *Phys. Rev. E* 61:5646–53
- Schmidt FG, Ziemann F, Sackmann E. 1996. Shear field mapping in actin networks by using magnetic tweezers. *Eur. Biophys. J.* 24:348–53
- Schmiedeberg M, Stark H. 2005. One-bead microrheology with rotating particles. *Europhys. Lett.* 69:629–35
- Schnurr B, Gittes F, MacKintosh FC, Schmidt CF. 1997. Determining microscopic viscoelasticity in flexible and semiflexible polymer networks from thermal fluctuations. *Macromolecules* 30:7781–92**
- Sickert M, Rondelez F, Stone HA. 2007. Single-particle Brownian dynamics for characterizing the rheology of fluid Langmuir monolayers. *Europhys. Lett.* 79:66005
- Slopek RP, McKinley HK, Henderson CL, Breedveld V. 2006. In situ monitoring of mechanical properties during photopolymerization with particle tracking microrheology. *Polymer* 47:2263–68
- Solomon MJ, Lu Q. 2001. Rheology and dynamics of particles in viscoelastic media. *Curr. Opin. Colloid Interface Sci.* 6:430–37
- Squires TM. 2008. Nonlinear microrheology: bulk stresses versus direct interactions. *Langmuir* 24:1147–59**
- Squires TM, Brady JF. 2005. A simple paradigm for active and nonlinear microrheology. *Phys. Fluids* 17:073101
- Sriram I, Furst EM, DePuit RJ, Squires TM. 2009. Small amplitude active oscillatory microrheology of a colloidal suspension. *J. Rheol.* 53:357–81
- Stark H. 2001. Physics of colloidal dispersions in nematic liquid crystals. *Phys. Rep.* 351:387–74
- Stark H, Ventzki D. 2001. Stokes drag of spherical particles in a nematic environment at low Ericksen numbers. *Phys. Rev. E* 64:031711
- Stark H, Ventzki D. 2002. Non-linear Stokes drag of spherical particles in a nematic solvent. *Europhys. Lett.* 57:60–66
- Starrs L, Bartlett P. 2003. Colloidal dynamics in polymer solutions: optical two-point microrheology measurements. *Faraday Discuss.* 123:323–34
- Stone HA, Ajdari A. 1998. Hydrodynamics of particles embedded in a flat surfactant layer overlying a subphase of finite depth. *J. Fluid Mech.* 369:151–73
- Sutherland W. 1905. A dynamical theory of diffusion for non-electrolytes and the molecular mass of albumin. *Philos. Mag.* 9:781–85
- Tseng Y, An KM, Wirtz D. 2002a. Microheterogeneity controls the rate of gelation of actin filament networks. *J. Biol. Chem.* 277:18143–50
- Tseng Y, Kole TP, Wirtz D. 2002b. Micromechanical mapping of live cells by multiple-particle-tracking microrheology. *Biophys. J.* 83:3162–76
- Tseng Y, Wirtz D. 2001. Mechanics and multiple-particle tracking microheterogeneity of alpha-actinin-cross-linked actin filament networks. *Biophys. J.* 81:1643–1656
- Tuteja A, Mackay ME, Narayanan S, Asokan S, Wong MS. 2007. Breakdown of the continuum Stokes-Einstein relation for nanoparticle diffusion. *Nano Lett.* 7:1276–81
- Vadas EB, Goldsmith HL, Mason SG. 1973. The microrheology of colloidal dispersions: the microtube technique. *J. Colloid Interface Sci.* 43:630–48

Concurrent with Mason et al. 1997b, introduces a real-space method for measuring the PSD of positional fluctuations of thermally excited probe particles, which are interpreted using a GSER.

This theoretical work introduces the challenges, and potential routes for their solution, in the emerging area of nonlinear microrheology.

- Valberg PA, Albertini DF. 1985. Cytoplasmic motions, rheology, and structure probed by a novel magnetic particle method. *J. Cell Biol.* 101:130–40
- Valentine MT, Dewalt LE, Ou-Yang HD. 1996. Forces on a colloidal particle in a polymer solution: a study using optical tweezers. *J. Phys. Condens. Matter* 8:9477–82
- Valentine MT, Kaplan PD, Thota D, Crocker JC, Gisler T, et al. 2001. Investigating the microenvironments of inhomogeneous soft materials with multiple particle tracking. *Phys. Rev. E* 64:061506
- Valentine MT, Perlman ZE, Gardel ML, Shin JH, Matsudaira P, et al. 2004. Colloid surface chemistry critically affects multiple particle tracking measurements of biomaterials. *Biophys. J.* 86:4004–14
- van Zanten JH, Amin S, Abdala AA. 2004. Brownian motion of colloidal spheres in aqueous PEO solutions. *Macromolecules* 37:3874–80
- Velegol D, Lanni F. 2001. Cell traction forces on soft biomaterials. I. Microrheology of type I collagen gels. *Biophys. J.* 81:1786–92
- Verhoeff AA, van Rijssel J, de Villeneuve VWA, Lekkerkerker HNW. 2008. Orientation dependent Stokes drag in a colloidal liquid crystal. *Soft Matter* 4:1602–4
- Verma R, Crocker JC, Lubensky TC, Yodh AG. 1998. Entropic colloidal interactions in concentrated DNA solutions. *Phys. Rev. Lett.* 81:4004–7
- Verma R, Crocker JC, Lubensky TC, Yodh AG. 2000. Attractions between hard colloidal spheres in semiflexible polymer solutions. *Macromolecules* 33:1770–86
- Waigh TA. 2005. Microrheology of complex fluids. *Rep. Prog. Phys.* 68:685–742
- Weihls D, Mason TG, Teitell MA. 2006. Bio-microrheology: a frontier in microrheology. *Biophys. J.* 91:4296–305
- Weitz DA, Pine DJ. 1993. Diffusing wave spectroscopy. In *Dynamic Light Scattering: The Method and Some Applications*, ed. W Brown, pp. 652–720. Oxford: Oxford Univ. Press
- Wilhelm C. 2008. Out-of-equilibrium microrheology inside living cells. *Phys. Rev. Lett.* 101:028101
- Wilkling JN, Mason TG. 2008. Optically driven nonlinear microrheology of gelatin. *Phys. Rev. E* 77:055101
- Willenbacher N, Oelschlaeger C. 2007. Dynamics and structure of complex fluids from high frequency mechanical and optical rheometry. *Curr. Opin. Colloid Interface Sci.* 12:43–49
- Willenbacher N, Oelschlaeger C, Schopferer M, Fischer P, Cardinaux F, Scheffold F. 2007. Broad bandwidth optical and mechanical rheometry of wormlike micelle solutions. *Phys. Rev. Lett.* 99:068302
- Wilson LG, Harrison AW, Schofield AB, Arlt J, Poon WCK. 2009. Passive and active microrheology of hard-sphere colloids. *J. Phys. Chem. B* 113:3806–12
- Wirtz D. 2009. Particle-tracking microrheology of living cells: principles and applications. *Annu. Rev. Biophys.* 38:301–26
- Wong IY, Gardel ML, Reichman DR, Weeks ER, Valentine MT, et al. 2004. Anomalous diffusion probes microstructure dynamics of entangled F-actin networks. *Phys. Rev. Lett.* 92:178101
- Xu JY, Viasnoff V, Wirtz D. 1998a. Compliance of actin filament networks measured by particle-tracking microrheology and diffusing wave spectroscopy. *Rheol. Acta* 37:387–98
- Xu JY, Palmer A, Wirtz D. 1998b. Rheology and microrheology of semiflexible polymer solutions: actin filament networks. *Macromolecules* 31:6486–92
- Xu K, Forest MG, Klapper I. 2007. On the correspondence between creeping flows of viscous and viscoelastic fluids. *J. Non-Newton. Fluid Mech.* 145:150–72
- Zhang W, Stone HA. 1998. Oscillatory motions of circular disks and nearly spherical particles in viscous flows. *J. Fluid Mech.* 367:329–58
- Ziemann F, Radler J, Sackmann E. 1994. Local measurements of viscoelastic moduli of entangled actin networks using an oscillating magnetic bead micro-rheometer. *Biophys. J.* 66:2210–16
- Zwanzig R, Bixon M. 1970. Hydrodynamic theory of velocity correlation function. *Phys. Rev. A* 2:2005–12



Contents

Singular Perturbation Theory: A Viscous Flow out of Göttingen <i>Robert E. O'Malley Jr.</i>	1
Dynamics of Winds and Currents Coupled to Surface Waves <i>Peter P. Sullivan and James C. McWilliams</i>	19
Fluvial Sedimentary Patterns <i>G. Seminara</i>	43
Shear Bands in Matter with Granularity <i>Peter Schall and Martin van Hecke</i>	67
Slip on Superhydrophobic Surfaces <i>Jonathan P. Rothstein</i>	89
Turbulent Dispersed Multiphase Flow <i>S. Balachandar and John K. Eaton</i>	111
Turbidity Currents and Their Deposits <i>Eckart Meiburg and Ben Kneller</i>	135
Measurement of the Velocity Gradient Tensor in Turbulent Flows <i>James M. Wallace and Petar V. Vukoslavčević</i>	157
Friction Drag Reduction of External Flows with Bubble and Gas Injection <i>Steven L. Ceccio</i>	183
Wave–Vortex Interactions in Fluids and Superfluids <i>Oliver Bühler</i>	205
Laminar, Transitional, and Turbulent Flows in Rotor–Stator Cavities <i>Brian Launder, Sébastien Poncet, and Eric Serre</i>	229
Scale-Dependent Models for Atmospheric Flows <i>Rupert Klein</i>	249
Spike-Type Compressor Stall Inception, Detection, and Control <i>C.S. Tan, I. Day, S. Morris, and A. Wadia</i>	275

Airflow and Particle Transport in the Human Respiratory System <i>C. Kleinstreuer and Z. Zhang</i>	301
Small-Scale Properties of Turbulent Rayleigh-Bénard Convection <i>Detlef Lohse and Ke-Qing Xia</i>	335
Fluid Dynamics of Urban Atmospheres in Complex Terrain <i>H. J. S. Fernando</i>	365
Turbulent Plumes in Nature <i>Andrew W. Woods</i>	391
Fluid Mechanics of Microrheology <i>Todd M. Squires and Thomas G. Mason</i>	413
Lattice-Boltzmann Method for Complex Flows <i>Cyrus K. Aidun and Jonathan R. Clausen</i>	439
Wavelet Methods in Computational Fluid Dynamics <i>Kai Schneider and Oleg V. Vasilyev</i>	473
Dielectric Barrier Discharge Plasma Actuators for Flow Control <i>Thomas C. Corke, C. Lon Enloe, and Stephen P. Wilkinson</i>	505
Applications of Holography in Fluid Mechanics and Particle Dynamics <i>Joseph Katz and Jian Sheng</i>	531
Recent Advances in Micro-Particle Image Velocimetry <i>Steven T. Wereley and Carl D. Meinhart</i>	557

Indexes

Cumulative Index of Contributing Authors, Volumes 1–42	577
Cumulative Index of Chapter Titles, Volumes 1–42	585

Errata

An online log of corrections to *Annual Review of Fluid Mechanics* articles may be found at <http://fluid.annualreviews.org/errata.shtml>